Near-edge X-ray absorption fine structure (NEXAFS) spectroscopy for mapping nano-scale distribution of organic carbon forms in soil: Application to black carbon particles

Johannes Lehmann,[1] Biqing Liang,[1] Dawit Solomon,[1] Mirna Lerotic,[2] Flavio Luizão,[3] James Kinyangi,[1] Thorsten Schäfer,[4] Sue Wirick,[2] and Chris Jacobsen[2]

Received 17 December 2004; accepted 3 January 2005; published 16 February 2005.

[1] Small-scale heterogeneity of organic carbon (C) forms in soils is poorly quantified since appropriate analytical techniques were not available up to now. Specifically, tools for the identification of functional groups on the surface of micrometer-sized black C particles were not available up to now. Scanning Transmission X-ray Microscopy (STXM) using synchrotron radiation was used in conjunction with Near-Edge X-ray Absorption Fine Structure (NEXAFS) spectroscopy to investigate nano-scale distribution (50-nm resolution) of C forms in black C particles and compared to synchrotron-based FTIR spectroscopy. A new embedding technique was developed that did not build on a C-based embedding medium and did not pose the risk of heat damage to the sample. Elemental sulfur (S) was melted to 220°C until it polymerized and quenched with liquid N_2 to obtain a very viscous plastic S in which the black C could be embedded until it hardened to a noncrystalline state and was ultrasectioned. Principal component and cluster analysis followed by singular value decomposition was able to resolve distinct areas in a black carbon particle. The core of the studied biomass-derived black C particles was highly aromatic even after thousands of years of exposure in soil and resembled the spectral characteristics of fresh charcoal. Surrounding this core and on the surface of the black C particle, however, much larger proportions of carboxylic and phenolic C forms were identified that were spatially and structurally distinct from the core of the particle. Cluster analysis provided evidence for both oxidation of the black C particle itself as well as adsorption of non-black C. NEXAFS spectroscopy has great potential to allow new insight into black C properties with important implications for biogeochemical cycles such as mineralization of black C in soils and sediments, and adsorption of C, nutrients, and pollutants as well as transport in the geosphere, hydrosphere, and atmosphere.

Citation: Lehmann, J., B. Liang, D. Solomon, M. Lerotic, F. Luizão, J. Kinyangi, T. Schäfer, S. Wirick, and C. Jacobsen (2005), Near-edge X-ray absorption fine structure (NEXAFS) spectroscopy for mapping nano-scale distribution of organic carbon forms in soil: Application to black carbon particles, *Global Biogeochem. Cycles*, *19*, GB1013, doi:10.1029/2004GB002435.

1. Introduction

[2] Organic carbon (C) in soil is the single largest pool of C on Earth's surface [*Watson et al.*, 2000] and controls much of its ecosystem services with respect to greenhouse gas emissions (of both C and N) and C sequestration, soil fertility and plant productivity, and filtration of water during its passage through soil [*Stevenson and Cole*, 1999]. Not only the total amounts of C are relevant for the biogeochemistry of C in soil, but also its forms. Black C has only recently been recognized as an important organic C pool in soils and sediments forming a continuum from partly charred organic materials to charcoal, coal, soot, and graphite [*Schmidt and Noack*, 2000]. Black C is found in any soil analyzed for black C contents [*Bird et al.*, 1999; *Schmidt et al.*, 1999; *Skjemstad et al.*, 2002; *Glaser and Amelung*, 2003], but questions remain about its residence time, alterations, and accumulation in terrestrial and aquatic systems [*Dickens et al.*, 2004; *Schmidt*, 2004]. Given that existing studies show both rapid [*Shneour*, 1966; *Bird et al.*, 1999] and slow [*Shindo*, 1991] rates of decomposition, it appears that a large part of black C is mineralized over short timescales, whereas a small part remains in a very stable, highly altered form displaying greater ^{14}C ages than the

[1]Department of Crop and Soil Sciences, Cornell University, Ithaca, New York, USA.
[2]Department of Physics and Astronomy, State University of New York at Stony Brook, Stony Brook, New York, USA.
[3]Instituto Nacional de Pesquisa da Amazonia INPA, Manaus, Brazil.
[4]Forschungszentrum Karlsruhe, Institute für Nukleare Entsorgung (INE), Karlsruhe, Germany.

0886-6236/05/2004GB002435$12.00

oldest soil organic matter fractions [*Pessenda et al.*, 2001]. The pool size of black C was successfully used to parameterize the inert organic matter pool of the RothC model of C turnover in soil [*Skjemstad et al.*, 2004], demonstrating that soil organic matter dynamics can be better described with an improved understanding of black C. While *Skjemstad et al.* [2004] successfully treated black C as an inert pool with respect to soil C dynamics, strong evidence suggests that nutrient dynamics are significantly influenced by black C [*Glaser et al.*, 2001; *Lehmann et al.*, 2003a], as, for example, *Sombroek et al.* [1993] found a greater cation exchange capacity in soils with larger proportions of black C. Important interactions exist between black C surfaces and inorganic as well as organic pollutants [*Ghosh et al.*, 2000; *Accardi-Dey and Gschwend*, 2002] and dissolved organic matter [*Pietikäinen et al.*, 2000] which are controlled by C forms on black C particles that influence, for example, hydrophobicity and surface charge. Abiotic oxidation and mineralization by microorganisms first occurs on surfaces of black C particles, and quantification of its extent will provide important information about the longevity of black C in the biogeosphere as well as the factors influencing its disappearance. Finally, the solubility of black C in water is highly dependent on the degree of surface oxidation [*Decesari et al.*, 2002] with consequences for transport in soil and water.

[3] Previous studies of black C were restricted to analyses of the properties of bulk black C isolates after oxidation of non-black C using ultraviolet (UV), thermal, or chemical oxidation [*Skjemstad et al.*, 1999; *Gelinas et al.*, 2001; *Masiello et al.*, 2002]. Surface properties of unaltered C forms, however, may be more relevant to the study of black C effects on soil biogeochemistry than bulk properties of isolates as pointed out above. Owing to the alterations during oxidative separation and the small size of black C particles [*Skjemstad et al.*, 1996], surface properties of black C have to our knowledge not been investigated up to now with respect to C compounds. Methods exist to study the morphology of single particles and their surfaces such as high-resolution transmission electron microscopy [*Palotas et al.*, 1996; *Gustafsson et al.*, 2001], to study certain C compounds such as PAH on black C using microprobe laser desorption and laser ionization mass spectrometry in 50-μm intervals or to identify C-rich patches in sediments using infrared analyses [*Ghosh et al.*, 2000]. Micro-raman spectroscopy and electron energy loss spectroscopy were used to characterize broad categories of C forms, but were restricted to single points of a particle [*Schmidt et al.*, 2002]. ^{13}C NMR was able to resolve nano-scale spatial associations between C forms but without the possibility to study spatial distributions in situ [*Skjemstad et al.*, 1997]. In contrast, the development of a method to characterize forms of C with high spatial resolution in sub-micrometer scale would, for example, allow the test of hypotheses that surface functional groups of black C particles significantly differ from those in the center of the black C particles, and that C on black C surfaces is more oxidized than at the center.

[4] Scanning Transmission X-ray Microscopy (STXM) using synchrotron radiation provides this opportunity to investigate nano-scale variations of C forms in soil through recent advances in X-ray microfocusing techniques [*Jacobsen et al.*, 2000; *Scheinost et al.*, 2001]. Using a tunable monochromator, Near-Edge X-ray Absorption Fine Structure (NEXAFS) can be obtained by increasing the photon energy through the absorption edge which is specific for each element and increases with atomic weight (284 eV for C) [*Stöhr*, 1992]. First, the core electron will be excited to the lowest unoccupied molecular orbital, while higher energy levels beyond the ionization threshold of C ($\sim$290 eV) will promote the core electron to continuum. The excited stages of the inner electron are characteristic for the geometric and electronic structure of the molecule and can be correlated to specific C forms [*Schäfer et al.*, 2003]. These features make NEXAFS using STXM a very sensitive technique to distinguish between, for example, aromatic-C, phenol-C, carbonyl-C, and carboxyl-C with a resolution of only several tens of nanometers and are ideal for the determination of very fine heterogeneity of C forms in soil.

[5] The challenge is to obtain thin sections with a thickness of around 100 nm that allow enough energy to penetrate the sample for detection. Since the objective of such an analysis would be to investigate functional groups of C, traditional C-based embedding materials cannot be used to obtain the thin sections as they interfere with high-resolution C analyses. This constraint excludes all materials that have commonly been used for embedding soil or geological materials such as resins and epoxy. In addition to water [*Ghosh et al.*, 2000], elemental sulfur (S) possesses unique properties that make it an appropriate material to embed samples that will be analyzed for C, since elemental S does not contain C, is liquid not too far above room temperature (melting point at 113°C), and is solid at room temperature. *Matrajt et al.* [2001] embedded micrometeorites in melted elemental S encapsulated in epoxy but were not interested in quantifying surface functional groups. A temperature of 100°C has been shown to significantly change C forms of humic substances [*Lu et al.*, 2001], and C organic chemistry on particle surfaces exposed to liquid elemental S with temperatures above 113°C may therefore change significantly, while C at the center of the particle is most likely not affected. *Bradley et al.* [1993] and *Flynn et al.* [2004] embedded interplanetary dust particles in elemental S by super-cooling small droplets of melted S that stay liquid for several seconds to hours below the melting point (L. Keller, personal communication, 2002). The droplets have to be very small to remain in this super-cooled liquid state, which requires the size of the embedded specimen to be in the micrometer range. Black C particles from biomass burning are usually several micrometers large and are therefore difficult to embed in droplets. Additionally, the crystalline nature of the sulfur droplets after solidification poses challenges for sectioning. These constraints required the development of a new embedding procedure to explore the opportunities provided by NEXAFS for soil organic matter studies.

[6] The objectives of this study were (1) to develop a new method to embed small black C particles for the investigation of their C forms using STXM and C(1s) NEXAFS spectroscopy and (2) to evaluate the suitability of NEXAFS

data and cluster analyses to distinguish between surface properties and different areas within the particles. NEXAFS data were compared with data obtained from synchrotron-based Fourier Transform Infrared (FTIR) spectroscopy, and the potential of the method for examining black C within global biogeochemical cycles is discussed.

2. Materials and Methods

2.1. Studied Organic Materials and Collection Sites

[7] Soil material was collected from different sites near Manaus, Brazil (3°8′S, 59°52′W, 40–50 m above sea level). The rainfall distribution in Manaus is unimodal with a maximum between December and May (204–298 mm per month; 73% of annual rainfall) and a mean annual precipitation of about 2088 mm, air temperature of 26.6°C, and atmospheric humidity around 84% [*Vose et al.*, 1992]. The natural vegetation is a tropical lowland rain forest. The studied soils are anthropic soils adjacent to naturally occurring Xanthic Hapludox [*Soil Survey Staff*, 1997] which are derived from Tertiary sediments. Samples from two sites were selected for this study: Hatahara and Donna Stella south of Manaus, Brazil, which had been influenced by human activity at around 1000 and 6000 years BP, respectively [*Neves et al.*, 2003; E. Neves, personal communication, 2003]. The soils were collected from the subsoil at depths of 0.43–0.69 m (Hatahara) and of about 1 m (Donna Stella) and have high proportions of biomass-derived black C [*Glaser et al.*, 2001], high total P (to 9064 mg kg^{-1}), and Ca (to 17545 mg kg^{-1}) concentrations typical for Amazonian Dark Earths [*Lehmann et al.*, 2003b]. For comparison, charcoal was obtained from wood of black locust (*Robinia pseudoacacia* L.) which was isothermically charred at 350°C for 40 min. NEXAFS spectra were also compared to non-black C of extracts from a Paleudalf from Ethiopia [*Solomon et al.*, 2005].

2.2. Preparation of Thin Sections

[8] Biomass-derived black C particles with diameters of 5–80 μm were separated from soil using super tweezers (N5, Dumont, Montignez, Switzerland) under a light microscope (30x; SMZ-10, Nikon, Japan). The representativeness of the particles studied here was verified visually for the two soils. Elemental sulfur (S) was chosen as the embedding medium for C NEXAFS spectroscopy as the embedding medium has to be free of C in order to not interfere with the C analyses. Elemental S was used with 99.9% purity (Fisher Scientific, Hampton, New Hampshire) (preferably in precipitated form and degassed to remove H_2S). The S was melted in a ceramic crucible on a hotplate at 220°C and remained at that temperature until it turned into a viscous and reddish-brown state (after about 2–3 min). Elemental S melts at 113°C, but S_8-rings open only above 159°C within a short period of time and form diradicals. The radicals then polymerize to form long chains (S_∞ polymers) resulting in an increase in viscosity [*Steudel and Eckert*, 2003]. The polymerization is important as it affects the properties of S after it is cooled. The viscous S was then poured into a mold lined with aluminum foil of a size that fitted into the sample holder of the ultramicrotome. In our case the designed mold was 15 mm long with a diameter of 8 mm and was fitted with a thread and bolt at the bottom to enable opening and removing the hardened S block from the mold with a rod. Immediately after the S was poured into the mold it was chilled by dipping it into liquid N_2 for 50–70 s. During rapid quenching, the S becomes amorphous (plastic S) but does not crystallize immediately [*Steudel and Eckert*, 2003]. The mold and frozen S was then left to warm under a dissecting microscope (10x, SMZ-140, Motic, China) for about 2–4 min. Condensed water was carefully wiped off the S block. During warming the amorphous and polymeric S gains a very viscous state (like soft chewing gum). Under the dissecting microscope, black C particles were carefully placed on top of the S and the S was pushed down with tweezers as soon as it reached the viscous state in order to move the black C particle into the S block. The optimum consistency for embedding only lasts for about 10–30 s, after which the amorphous S converts to a microcrystalline but still plastic state. The contact of S and particle could be improved by using a hot iron pen under N_2 gas flow for 2 min.

[9] The S block with the embedded particle is transferred to a light microscope (30x) and trimmed with a razor blade to an optimum trapeze shape for sectioning with the black C in the middle. The plastic consistency of the S block is meta-stable for 6–10 hours after embedding, after which it returns to the orthorhombic state (α-S_8 allotrope) and could not be cut very well. Sectioning to a thickness of 200 nm was done with an ultramicrotome (Ultracut UTC, Leica Microsystems Inc, Bannockburn, Illinois) using a glass knife for trimming and a diamond knife (MS9859 Ultra 45°C, Diatome Ltd., Biel, Switzerland) for final cutting at 1.2 mm s^{-1} (cutting angle of 6°) (thinner sections of about 100 nm are desirable, but are more difficult to obtain). The receiving trough was filled with water, and the floating sections were transferred to a Cu grid using a loop. Copper grids that did not contain C (200 mesh, silicon monoxide 53002, Ladd Research, Williston, Vermont) were used to improve signal-to-noise ratios. Before measurement of the sections, the remaining S around the sections was removed from the grids by sublimation in a vacuum oven (40°C, −31 bar) for 1 hour.

2.3. Data Acquisition of Carbon Forms

2.3.1. NEXAFS Using Scanning Transmission X-ray Microscopy

[10] Near-edge X-ray absorption fine structures (NEXAFS) were obtained using Scanning Transmission X-ray Microscopy (STXM) at beamline X1A1 of the National Synchrotron Light Source at Brookhaven National Laboratory. This beamline produces a soft X-ray beam from the 2.8 GeV electron storage ring and illuminates a monochromator that is tunable over 250 to 800 eV. A Fresnel zone plate focuses the X-rays on the sample. Slits were set to 40/25/25 μm to give an energy resolution of 0.1 eV. Under the given slit setup and zone plate used, the maximum spatial resolution is ~50 nm. The STXM can be operated to obtain spectra at one particular spot of the sample or to obtain maps of a sample at one or multiple energy levels (the latter is also referred to as stacks). We

acquired the so-called stacks of entire samples by taking images at different energy levels across the absorption edge, and aligned them using cross correlation. The monochromator energy was increased from 280 to 282.5 eV in 0.3-eV steps (dwell time 1 ms), to 292 eV in 0.1-eV steps (dwell time 3 ms), and to 310 eV in 0.3-eV steps (dwell time 3 ms). Smaller energy steps were chosen at levels where core electrons of C are excited (285–290 eV). The dwell time was increased to improve counting statistics (reduce error) at spectroscopically interesting regions, in regions where samples showed high absorbance, or in regions where the incident flux is low.

2.3.2. Fourier Transform Infrared (FTIR) Analyses

[11] Fourier Transform Infrared (FTIR) analysis was done at the beamline U10B of the National Synchrotron Light Source at Brookhaven National Laboratory. The beamline is equipped with a Spectra Tech Continuum IR microscope fitted with 32x transmission/reflection and FTIR step-scan spectrophotometer (Nicolet Magna 860, Thermo Nicolet Corporation, Wisconsin) with a KBr beam splitter and mercury-cadmium-telluride (MCT) detector with 500–4000 cm^{-1} frequency range and 1.0 cm^{-1} spectral resolution. Spectra of the center of particles from Donna Stella soil were recorded with a 10-μm aperture size from 4000 to 650 cm^{-1} with a resolution of 4 cm^{-1}. Each spectrum was composed of 512 scans co-added before Fourier transform processing. For comparison, fresh charcoal and particulate organic matter of adjacent soil with negligible black C was measured in KBr pellets using 64 scans.

2.4. Data Analyses

[12] Individual maps of all energy levels measured were stacked using Stack_Analyze software (C. Jacobsen, SUNY Stony Brook; built on IDL software, Research Systems Inc., Boulder, Colorado). Before spectral analysis, an alignment is necessary as the sample can drift substantially throughout the scan. Maps were aligned by using the map at 290 eV as a reference, since most of the spatial features are well expressed at that energy level, and was repeated until the shift was less than 0.3 pixels. The spectra for each point are then reconstructed over the entire region of the aligned stack [*Jacobsen et al.*, 2000]. An area in sufficient distance from the sample (checked for all energy levels) was defined for background correction (I0). Principal component and cluster analysis was performed with PCA_GUI 1.0 [*Lerotic et al.*, 2004] to orthogonalize and noise-filter the data and to classify regions in the sample according to spectral similarities. Analyses with increasing numbers of components and clusters were run to test for robustness of the results. The first component was included in the analyses. Subsequently, Singular Value Decomposition (SVD) was performed to calculate target maps and corresponding fitted target spectra from the spectra obtained by cluster analysis. Those target maps which did not show spatial patterns but were merely randomly distributed were successively removed from the analysis until only target maps with nonrandom distribution of spectral characteristics remained. Spectra from the clusters and target maps were smoothed 3 times using Spectra_gui 0.99 (SUNY Stony Brook).

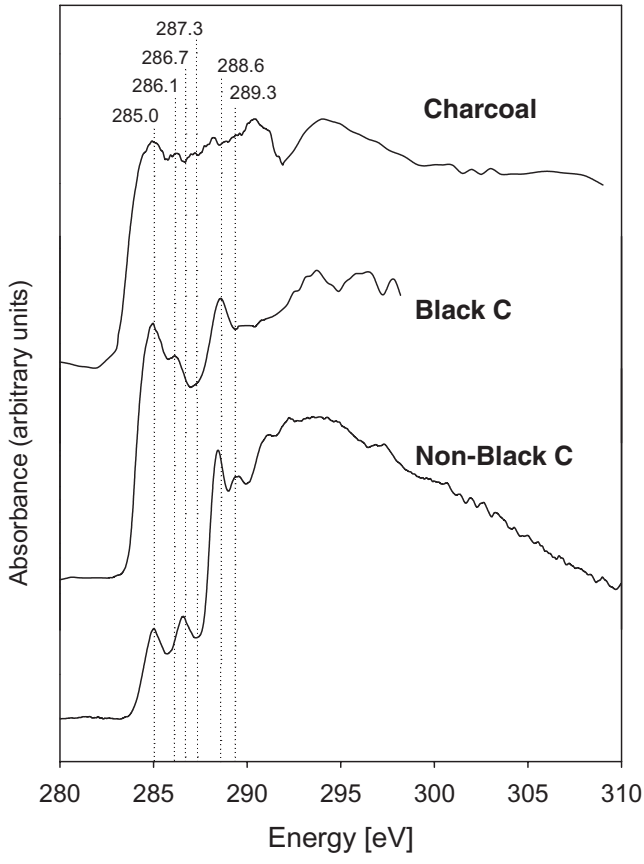

Figure 1. C(1s) NEXAFS spectra of charcoal (*Robinia pseudacacia* L.), a black C particle (from Donna Stella soil), and a non-black C (non-black C is a soil extract from *Solomon et al.* [2005]).

[13] The spectra were deconvoluted using arctangent function for the ionization step at 290 eV with a full-width half maximum (FWHM) of 0.4 eV to generate a continuum of the spectrum up to 294 eV. The FWHM of the Gaussian peaks (G) was set at 0.4 eV, and six Gaussian functions representing the main 1s-π* transitions at 284.3 (G1), 285.1 (G2), 286.5 (G3), 287.3 (G4), 288.4 (G5), and 289.3 (G6) eV and 2 s higher (1s-2π*) transitions at 289.1 and 289.7 eV (data not shown) were resolved [*Cody et al.*, 1998; *Scheinost et al.*, 2001; *Schäfer et al.*, 2003]. Additionally, two Gaussian peaks for σ* transitions (σ^1 and σ^2) were simulated with FWHM of <1 and <2 eV using WinXAS version 3.0 (T. Ressler, Berlin). Since the fine structure in the C NEXAFS region above 290 eV transitions were very broad [*Cody et al.*, 1998; *Schäfer et al.*, 2003], only the main 1s-π* transitions were used for subsequent quantification and interpretation of the C (1s) NEXAFS results. The fit for the highly aromatic C was not satisfactory, and therefore only data for regions of more oxidized C were presented here. For the qualitative analyses of C forms from the FTIR spectra, we subtracted the background of the Cu grid or KBr window, automatically corrected the baseline, and smoothed the spectra, identified the peaks, and normalized the spectra on a reduced portion of the wave

Table 1. Peak Assignment for C Forms Obtained From C (1s) NEXAFS and FTIR Spectroscopy

Energy Level	Carbon Forms[a]
	C (1s) NEXAFS, eV
284.3	quinone-C, protonated aromatic-C
284.9–285.5	protonated/alkylated to carbonyl-substituted aromatic-C
286.1	unsaturated C
286.7	phenol-C, ketone C=O
287.1–287.4	aliphatic-C, aromatic carbonyl
287.7–288.6	carboxyl-C, C=O, COOH, CH_3, CH_2, CH
289.3	carbonyl-C, alcohol
	FTIR, cm^{-1}
3411, 3339, 3192	OH stretching vibrations of H-bonded hydroxyl (O-H) groups of phenols with traces of amine stretches (N-H)
3077	CH from aromatic-C [*Smith and Chughtai*, 1995; *Ghosh et al.*, 2000]
2922	weak CH_3 stretch vibrations of aliphatic-C
2856	weak CH_2 stretch vibrations of aliphatic-C
1710–1690	C=O stretching mainly of carboxyl-C and traces of ketons and esters [*Koch et al.*, 1998; *Pradhan and Sandle*, 1998]
1630	C=O conjugated ketons and quinones [*Haberhauer et al.*, 1998; *Koch et al.*, 1998]
1595	C=C of aromatic-C [*Guo and Bustin*, 1998; *Haberhauer et al.*, 1998]
1513	CH or NH bending, characteristic of undecomposed litter [*Haberhauer et al.*, 1998]
1433	CH_2 bending [*Smith and Chughtai*, 1995]
1393	CH deformation of aliphatic-C (some C-O stretching of phenolic OH)
1257	C-O stretching and OH deformations of carboxyl-C
1115	OH of carboxyl-C [*Pradhan and Sandle*, 1998]
1037	C-O stretching of polysaccharides [*Haberhauer et al.*, 1998]

[a]Peak assignments for NEXAFS according to *Cody et al.* [1998], *Schäfer et al.* [2003], and own observations and for FTIR according to references indicated (others: *Haberhauer et al.* [1998] and *Smith and Chughtai* [1995]).

numbers (4000 to 750 cm^{-1}) using OMNIC v.6.1 (Thermo Electron Corp., Woburn, Massachusetts).

3. Results

3.1. Point Spectra of Black C and Non-black C

[14] Carbon NEXAFS was able to resolve clear differences between C forms of black C and non-black C. Spectra of a soil with little or no black C (non-black C in Figure 1) showed low amounts of aromatic (sum of quinone and protonated aromatic-C around 285.0 eV) and phenol-C (286.7 eV), but large amounts of carboxyl-C (288.6 eV; Table 1). In contrast, biomass-derived black C in the form of charcoal without exposure to soil was highly amorphous with a dominant peak in the aromatic region (285.0 eV). Black C that was deposited about 6000 years BP (Donna Stella soil) in a covered soil profile maintained the dominance of aromatic C, but the spectrum was better resolved than the one of fresh charcoal, and a distinct peak in the carboxylic region is visible.

[15] FTIR spectra were obtained from a black C particle and non-black C particle mixture of Donna Stella soil as well as fresh charcoal (Figure 2). Especially in fresh charcoal, a dominant band was expressed at around 1590 cm^{-1}. The bands assigned to asymmetric and symmetric aliphatic groups (CH_3 at 2922 cm^{-1}, CH_2 at 2856 cm^{-1}, C-H of aliphatic groups at 1393 cm^{-1}; Table 1) as well as the band attributed to C-O stretching vibrations of polysaccharides (1034 cm^{-1}) were smaller in black C and fresh charcoal than in non-black particles (Figure 2). Also the bands from C-O stretching and OH deformation and from H-bonded hydroxyl (O-H) and amine (N-H) groups were weakly resolved in black C.

3.2. Principal Component and Cluster Analysis of Cross-Sectional Maps of Black C

[16] Cluster analysis and preceding principal component analyses were explored using several combinations of a number of components and clusters using a black C particle from Hatahara soil (Figure 3). Spatial distribution of clusters was not significantly affected by increasing the number of principal components (compare 2/4, 3/4, and 4/4 in Figure 3). Beyond two principal components, no new features appeared. Increasing the number of clusters, however, changed the shape of the distribution of C forms (Figure 3). While the shape of clusters changed by increasing the number of clusters, the general trend of spectral properties remained the same between clusters (Figures 4a–4c). The aromaticity (at lower eV) decreased from the inside to the outside of the particle irrespective of the number of clusters. With more clusters, however, the difference between the C forms on the outside and inside became more apparent.

[17] Target maps were constructed from cluster spectra for all analyzed combinations of principal component and cluster analyses (2/4, 3/4, 4/4, 4/6, 4/10 in Figure 3), but differed only marginally in their spatial composition (target maps only shown for 4/4, 4/6, 4/10 in Figure 3). Irrespective of the number of principal components or clusters, the number of target maps with recognizable features that were not randomly distributed was always three. More than three target maps were not useful. In contrast to the spatial distribution of similar C forms, the RMS error of the target spectra significantly depended on the number of principal components or clusters. With few components (less than three) and few clusters (less than four), mean square errors for target spectra were high (>0.01), and decreased when more components were used in the analysis to <0.01 (less

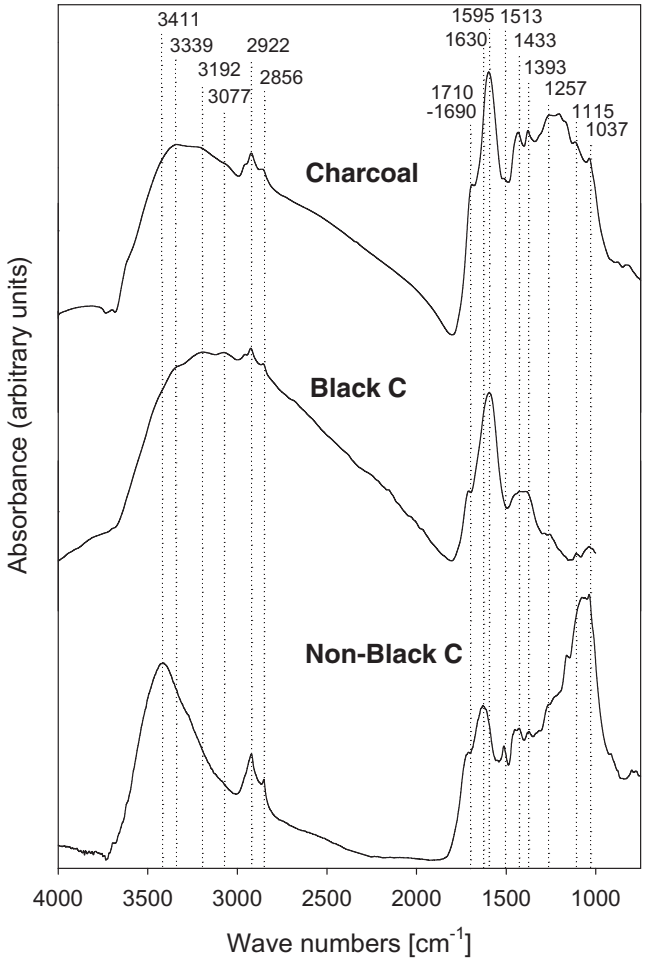

Figure 2. FTIR spectra of charcoal (*Robinia pseudacacia* L.), a black C particle, and a non-black C particle mixture (both from Donna Stella soil); numbers above the peaks indicate wave numbers attributed to specific C-stretches explained in the text.

with more clusters using fewer than four components). More than four components and six clusters did not reduce the errors further. In contrast to the error of the target spectra, the spatial distribution of functional groups did not change with fewer components (Figure 3). The spectral signature of the three target maps changed slightly as a function of the number of clusters largely related to the reduction in error (target spectra only shown for 4/6 in Figure 4). For our particle, an optimum of four components and six clusters was found based on the error reduction.

3.3. Carbon Forms on Black C Surfaces

[18] The center cluster of both black C particles from different soils analyzed here had very similar spectral characteristics (Figures 1 and 4). The spatial analysis of the black C particle successfully revealed a progressive oxidation of black C from the surface with a significant reduction of aromatic C and a proportional increase of carboxylic C (Figure 4). Progressing oxidation did not penetrate the particle uniformly, but more oxidation was observed at the lower than the upper end of the particle (Figures 3 and 5). Singular Value Decomposition and the target maps and spectra (Figure 5) confirmed the results of the cluster analysis since target spectra were derived from principal components: A highly aromatic core is surrounded by more oxidized C forms. However, additional aspects of the spatial features became apparent from the target maps. Three chemically and morphologically distinct regions

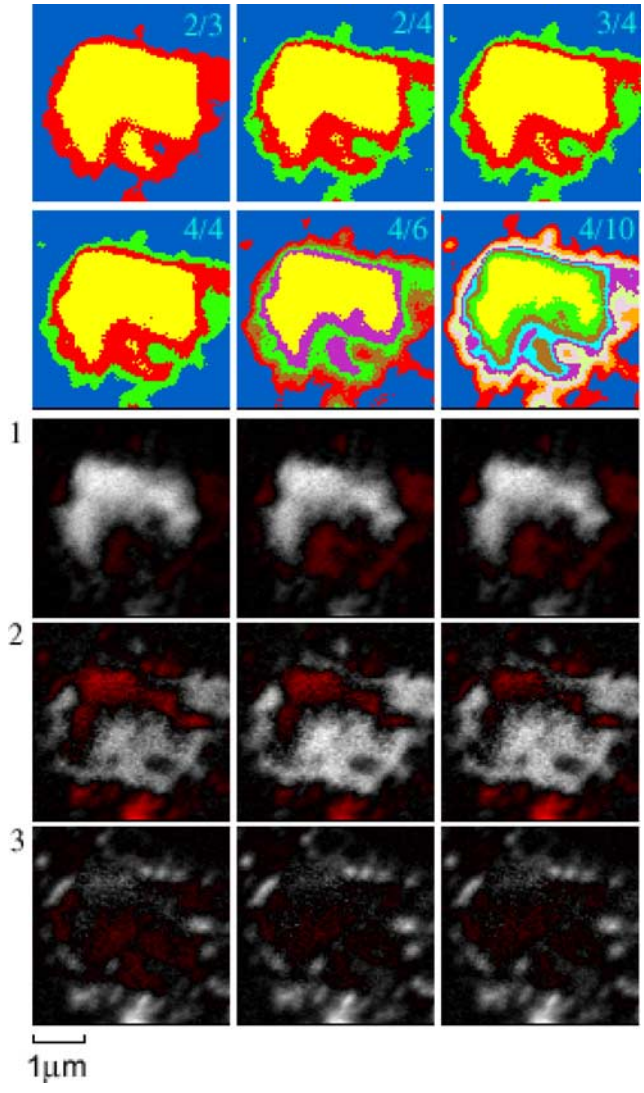

Figure 3. Cross-sectional stacked maps of similar C forms obtained from principal component and cluster analyses (top plots, labeled 2/4–4/10) and target maps obtained from singular value decomposition (bottom rows, labeled 1–3) of a black C particle (from Hatahara soil); 2/4 signifies the computation of maps by using two components and four clusters; target maps were only shown for cluster analyses with four components and four, six, or ten clusters (i.e., 4/4, 4/6, and 4/10); singular value decomposition yielded three target maps regardless of the number of components or clusters used.

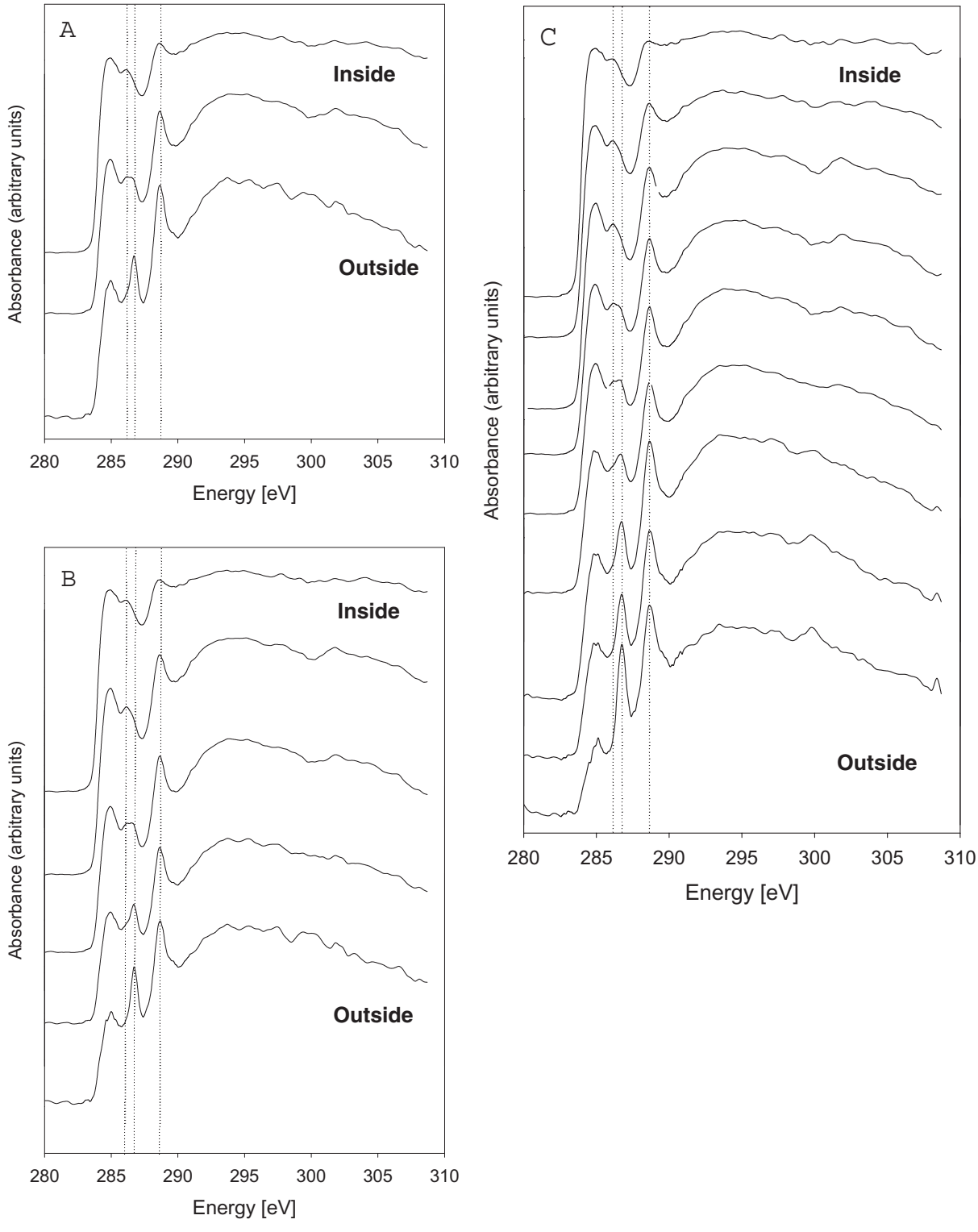

Figure 4. C(1s) NEXAFS cluster spectra of a black C particle (from Hatahara soil) by computing three different principal component analyses with four components and either (a) four, (b) six, or (c) ten clusters; cluster spectra organized from inside to outside of the particle corresponding to clusters in Figure 3 (Figure 4a: 4/4; Figure 4b: 4/6; Figure 4c: 4/10); vertical dotted lines indicate energy levels of 286.1, 286.7, and 288.6 eV indicative of unsaturated, phenolic, and carboxyl-C, respectively (Table 1).

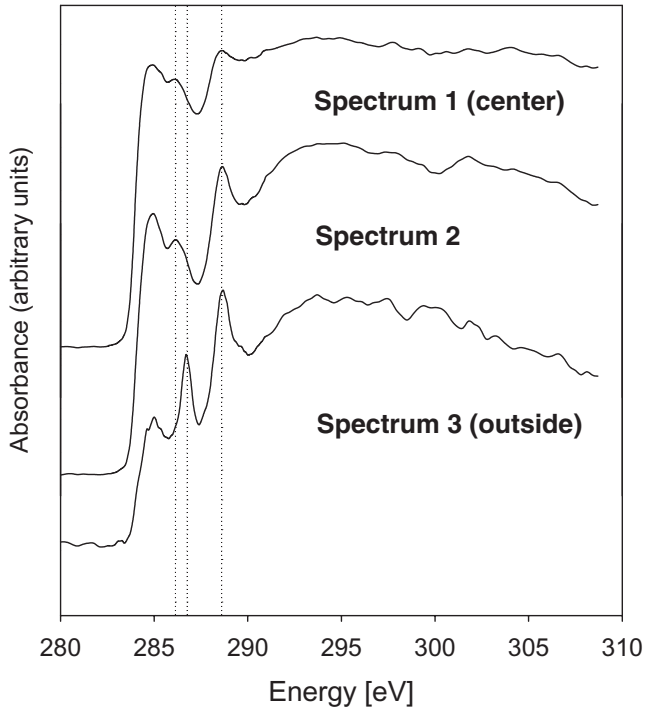

Figure 5. C(1s) NEXAFS spectra of target maps of a black C particle (from Hatahara soil) (maps 1–3 from cluster analysis 4/6 of Figure 3); vertical dotted lines indicate energy levels of 286.1, 286.7, and 288.6 eV indicative of unsaturated, phenolic, and carboxyl-C, respectively (Table 1).

appeared in the cross section of the black C particle in contrast to the cluster analysis. While the aromatic core was similar (with about 29% carboxyl and carbonyl C; see section 2 for explanation of uncertainties), relatively highly oxidized C (with 42% carboxyl and carbonyl) on the soil surface appeared to be concentrated in spots and not be a contiguous layer as the clusters suggested.

4. Discussion

4.1. Embedding of Single Soil Organic Particles

[19] The developed embedding technique proved feasible for sample preparation that requires thin sections for transmission spectroscopy of C forms within micrometer-scale particles. This is a significant advancement over traditional embedding procedures that use resins, epoxy, paraffin, or other binding agents which are all C-based and would interfere with the C measurement. Experiments using water as an embedding medium and subsequent cryo-sectioning [*Ghosh et al.*, 2000] did not provide an advantage over the method using elemental S in our study, although combinations may offer opportunities for larger particles or aggregates. During embedding in elemental S, the samples were not subjected to heat above room temperature which makes the method suitable for organic materials that change their properties at higher temperatures. Already temperatures below 100°C, and therefore below the melting point of elemental S, can cause significant alterations of organic matter structures of humic substances [*Lu et al.*, 2001]. If the objective of a study is to compare the functional groups on the surface with those at the center of particles, the surfaces must not come into contact with melted and hot elemental S. In the S droplet method used by *Flynn et al.* [2004] and only briefly described by *Bradley et al.* [1993], particles are embedded into a super-cooled S droplet at room temperature (droplets remain liquid for a short period of time if they are sufficiently small (L. Keller, personal communication, 2002)) which works well for micrometer-size particles, but is less suitable for particles larger than 20 μm.

[20] The time-consuming nature of both the embedding and the following spectroscopic techniques is prohibitive to the analysis of a large number of particles. This means that inferences about biogeochemical processes in soil or elsewhere have to be made from a limited number of observations. This is a constraint that has to be accepted not only for methodological reasons but also for reasons of the hypothesis tested. If the objective is to quantify changes of chemical properties at extremely small scales, those observations are necessarily restricted to a small spatial area in the sample and may only be representative to a very small area in soil due to the inherent heterogeneity of soil properties. Special attention has to be paid to the representativeness of the studied particles, which can be ensured using appropriate optical identification and sampling methods.

4.2. Advances in Principal Component Analyses of Small-Scale Carbon Distributions

[21] The principal component analysis provided the unique opportunity to map the distribution of C forms for entire organic particles according to spectral similarities. This is a significant advancement for several reasons: (1) Organic matter in soil (as in many other environmental or biological systems) is very complex and the analysis of single spectral characteristics such as aromaticity may not provide comprehensive information about biogeochemical processes and (2) the thickness within the section may inevitably vary, and absolute concentration of specific C forms may be biased.

[22] The spatial analysis of clusters and target maps was very robust with respect to the choice of numbers of components, clusters, and target spectra. Therefore the results more likely represent true differences in organic composition rather than random distributions dependent on the analyst. Target maps revealed very interesting spatial features such as the noncontiguous layer of the most oxidized C at the surface of black C particles that were not apparent in the cluster analysis (Figure 3). Quantitative information, however, through spectral deconvolution proved difficult for black C particles, especially for areas with high proportions of aromatic C, and require further experimentation.

4.3. Opportunities for the Study of Carbon Chemistry of Black Carbons

[23] The spectral properties showed clear chemical characteristics that were significantly different between black C and non-black C highlighting the appropriateness

of NEXAFS for black C studies. The bulk properties of the studied black C particles from biomass burning remained aromatic even after several thousand years of exposure in soil. Their spectral signatures still resembled those of charcoal (Figure 1) and were similar between black C obtained from different soils (Figures 1 and 3). While similar spectral signatures strongly indicate similar C structures, it cannot be excluded that the proportion of some forms of C (e.g., aliphatic C) is changing without a clear spectral response. In comparison, non-black C is much more oxidized (Figure 1). High aromaticity of black C is well documented for black C obtained after separation by UV oxidation [*Skjemstad et al.*, 1999]. In previous studies, however, no information was given about the age of the black C in soil in conjunction with chemical properties. It is generally assumed that black C is highly stable in soil [*Schmidt and Noack*, 2000], but actual data are scarce and often contradictory [*Shneour*, 1966; *Shindo*, 1991; *Bird et al.*, 1999].

[24] Despite the fact that black C is defined as a highly aromatic organic matter, the degree of aromaticity may vary according to the origin of the black C and environmental exposure [*Schmidt and Noack*, 2000]. The spectral signatures from the center of our black C particles very closely resembled an example of a charcoal particle. However, the surfaces and even large parts of the areas inside the particle differed significantly in their chemical signature from areas at the center or from the charcoal particle. These areas were much more oxidized and would probably be removed by any oxidative separation procedure using UV, high temperature, or dichromate. The present method enables direct detection and visualization of such differences at nano-scale for intact black C particles which was not available up to now.

[25] A prominent absorption that can be assigned to aromatic C bonded to oxygen [C(1s) $\rightarrow \pi^*_{C-OH}$] as found in phenol or halogenated aromatics is located at 286.5 eV [*Cody et al.*, 1995]. Deconvolution procedures were successfully applied to spectra of isolated hydrophilic organic compounds (humic or fulvic acids) to quantify the amount of phenol-type groups using this 286.6-eV transition [*Cody et al.*, 1998; *Scheinost et al.*, 2001; *Schäfer et al.*, 2003; *Solomon et al.*, 2005]. The hydroxylation associated with aromatic C usually found in groundwater fulvic acids derived from brown coal intercalations [*Schäfer et al.*, 2005] or in sub-bituminous B rank coal [*Cody et al.*, 1995] indicates an average hydroxylation of two hydroxyl groups per aromatic ring.

[26] Crystalline graphite structures, on the other hand, exhibit a broad absorption in the 285–286 eV range comparable to the features observed in the charcoal and black C spectra (Figures 1, 4, and 5), whereupon the intensity of this π band ($1\pi^*_{C=C}$ transition) strongly depends on the amount of associated hydroxyl groups [*Francis and Hitchcock*, 1992] and the crystallinity of the material [*Denley et al.*, 1980; *Comelli et al.*, 1988; *Braun et al.*, 2004]. Similar X-ray absorption features with strong absorption peaks in the energy region of 285.9eV and 286.2eV were also found in the fullerene molecule C_{60} [*Luo et al.*, 1995]. On the basis of these observations, we interpret the observed spectral feature at 286–286.1 eV in the charcoal and black C spectra (Figures 1, 4, and 5) as π^* resonance characteristic for unsaturated (*sp* or sp^2) C bonds and not as resonance from aromatic C bonded to oxygen [C(1s) $\rightarrow \pi^*_{C-OH}$]. The peak at 286.7 eV observed in the non-black C and the outer region is most likely generated by an abundance of phenolic C.

[27] The carboxylic peak showed small shifts for the black C and non-black C (Figure 1) which hints at the presence of different types of carboxylic C compounds as found for formic acid, acetic acid, or propionic acid to be in the range from 288.2 to 288.6 [*Cody et al.*, 1998; *Schäfer et al.*, 2003; *Scheinost et al.*, 2001]. This shift was found to a lesser extent between regions within the black C particle.

[28] For aromatic rings or solids, a structureless broad σ^* feature is usually observed owing to the interaction of adjacent bonds causing a splitting of resonances through conjugation or long-range band formation. In the charcoal and black C spectra of Figure 1, structures appear in the σ^* region (>291 eV), indicating an increase in structural order. Similar findings were observed by annealing amorphous or hydrogenated amorphous C to graphitic C [*Wesner et al.*, 1983; *Comelli et al.*, 1988] and with the increase of chain length in polyacenes [*Agren et al.*, 1995]. The lack of pronounced structures in the σ^* region of the spectra from the inner area of the black C (Figures 4 and 5) indicates no unique short- or long-range order. This can be interpreted as either a heterogeneous matrix with a partly well-defined structure in the form of, for example, small crystallites or a homogeneous matrix without long-range periodicity.

[29] Chemical fingerprints obtained from FTIR spectroscopy were less characteristic for black C than those from NEXAFS spectroscopy. NEXAFS showed clear differences between black C and non-black C in our study (Figure 1) and in comparison to non-black C from other studies of humic acid extracts [*Scheinost et al.*, 2001; *Schäfer et al.*, 2003] or natural organic colloids [*Schäfer et al.*, 2003]. FTIR spectra of black C, however, were not as specific compared to non-black C (Figure 2), partly owing to the overlap of bands attributed to carboxyl-C and aromatic C between 1700 and 1550 cm^{-1}. While the stretch at 1590 cm^{-1} is characteristic for black C, i.e., charcoal, soots, and coal [*Smith and Chughtai*, 1995; *Guo and Bustin*, 1998; *Koch et al.*, 1998], the peak assignment is not unambiguous and can include significant amounts of conjugated carbonyl-C [*Smith and Chughtai*, 1995; *Pradhan and Sandle*, 1998]. However, bands characteristic of carboxyl-C in non-black organic matter appear at 1750–1600 cm^{-1}, whereas carboxyl-C seems to be the source of the strong absorption band at 1595 cm^{-1} in our samples.

[30] Black C appears to show low absorbance of OH stretch vibrations around 3400 cm^{-1} compared to non-black C (Figure 2). Soot particles obtained from sediments were identified by a peak at 3000–3100 cm^{-1} [*Ghosh et al.*, 2000] which was only weakly expressed in our sample. Similarly, *Braida et al.* [2003] did not describe a characteristic peak indicative of aromatic C in contrast to their NMR analyses of charcoal. Spectral characteristics indicative of low carbohydrate contents (1034 cm^{-1}) were consistent with expectations for black C in Donna Stella

soil and fresh charcoal compared to non-black C, but were also found in some humic substance extracts of non-black C where higher carbohydrate concentrations than in black C could be expected [*Chen et al.*, 2002; *Solomon et al.*, 2005].

[31] Given the lower spatial resolution of FTIR (maximum 8–10 μm) and the ambiguity to distinguish between aromatic and carboxylic-C in the region between 1800 and 1500 cm^{-1}, it appears that FTIR is less suitable than NEXAFS for assessing oxidation of black C on surfaces and across sections of particles in complex natural systems. However, even NEXAFS using STXM may not be able to resolve spatial distribution in particles that are smaller than 500 nm such as most soot black C [*Braun et al.*, 2005].

4.4. Carbon Forms on Black Carbon Surfaces and Implications for Biogeochemical Cycles

[32] STXM and NEXAFS followed by principal component analysis provided the opportunity to distinguish between three spatially and chemically distinct regions in a black C particle: a highly aromatic core, a progressively more oxidized region partly surrounding the core, and a noncontinuous region surrounding the two former areas that showed higher carboxylic and phenolic than aromatic and unsaturated C signatures (Figures 3 and 5). The central region may correspond to a weakly altered black C material that resembles the original material more than the other two areas. The second region is most likely also derived from the original black C particle, but has been progressively altered through microbial and abiotic oxidation in soil. Despite the fact that highly aromatic forms of black C are very stable, they can be mineralized over long periods of time [*Schmidt and Noack*, 2000]. Direct evidence exists that microbes can metabolize black C, as microbial cell wall material in soils containing a high proportion of lignite displayed a radiocarbon age strongly influenced by that of the coal [*Rethemeyer et al.*, 2003]. Also, wood and leaf decaying fungi have been shown to degrade brown coal [*Hofrichter et al.*, 1999].

[33] The spatial attributes of the surrounding and outer region resolved by STXM may suggest that it is not composed of oxidized organic matter derived from the black C particle itself but of adsorbed organic matter. It only consists of about 25% aromatic C, but 42% carboxyl and carbonyl C as determined by spectral deconvolution (see section 2 for uncertainties in deconvolution). While the observed changes in C functionality provide evidence for this conclusion, it cannot be excluded that changes in aliphatic C structures occurred that were not detectable by NEXAFS. Dissolved organic matter adsorbs strongly to black C [*Pietikäinen et al.*, 2000], and activated C has shown to sorb microorganisms, and this adsorption was increased with higher hydrophobicity [*Rivera-Utrilla et al.*, 2001]. The most likely explanation of the more oxidized regions surrounding the particle in spots rather than in a contiguous area is adsorption of non-black C in the form of humified macromolecules or microbes. The observed phenolic peak at 286.7 eV in the outer region and the presence of the unsaturated C peak at 286.1 eV in the two inner regions provide evidence for a different origin of the two more oxidized parts of the studied particle. Further experiments will be necessary to test this hypothesis.

[34] The spatial and chemical features shown here would not be detectable in bulk analyses of black C isolates using, for example, solid-state ^{13}C NMR, because these oxidized features constitute only a small proportion of the total mass of the black C in soil and NMR does not at present provide the opportunity to map cross-sectional areas of micro-scale particles. Since the relatively highly oxidized portions of the black C particle or its adsorbates were located on the surface, a higher degree of oxidation than an assumed dominance of aromatic C should actually have a significant effect on how black C affects biogeochemical cycles in soil. Results may be related to the high cation exchange capacity found in certain anthropogenic soils that have very high black C concentrations [*Sombroek et al.*, 1993]. This would mean that black C significantly contributes to the retention of cations including toxic metals as well as plant nutrients with implications for contaminant movement and soil fertility. Other implications derived from the use of STXM and NEXAFS include better estimates for black C mineralization which may fill an important gap in the understanding of global black C cycles [*Schmidt*, 2004]. Understanding the factors controlling black C mineralization would help explain the disparity between a high production of black C in terrestrial systems through biomass burning [*Kuhlbusch and Crutzen*, 1995] and a low accumulation in oceans [*Dickens et al.*, 2004] with still uncertain rates of transport from terrestrial ecosystems to the oceans [*Mitra et al.*, 2002]. This technique may also open new avenues for fingerprinting different types of black C particles in the environment. It is widely acknowledged that black C has no clearly defined properties due to different production conditions [*Schmidt and Noack*, 2000]. It also has different properties as an effect of biochemical aging in the environment, for which the proposed method will allow new insights. Knowledge about specific chemical characteristics and their nano-scale distribution may help in determining the origin of particles and their behavior in soil.

5. Conclusions

[35] For the first time the submicrometer spatial heterogeneity of organic C forms of small particles in soil and specifically of black C was demonstrated, which required the development of a new sample preparation technique. This new approach of embedding micro-scale samples in elemental S that was melted and rapidly chilled provided the opportunity to quantify nano-scale distribution of C forms without contamination from a C-based embedding medium and without the risk of heat damage to the sample surfaces. This technique was used for C(1s) NEXAFS spectroscopy in conjunction with STXM as well as FTIR using synchrotron radiation but is applicable to any analytical method that requires transmission spectroscopy of C forms. Such an analytical tool proved invaluable for detecting significant variations of C forms within a black C particle. An example showed large

differences between a highly aromatic core to a strongly carboxylated surface. Cluster analyses provided evidence for biochemical oxidation of the black C particle itself as well as for adsorption of non-black C. Such differences have important implications for biogeochemical cycles of nutrients or C in soil as black C was considered inert and only adsorbing unpolar or less polar substances. This technique will also help in understanding mineralization and movement of black C itself in order to fill an important gap in our understanding of global biogeochemical cycles of C.

[36] **Acknowledgments.** This project was funded by the Department of Crop and Soil Sciences at Cornell University and by the National Science Foundation Ecosystem Cluster under contract 46028/A001. The NEXAFS spectra were obtained at the National Synchrotron Light Source (NSLS), Brookhaven National Laboratory, at the beamline X-1A1 developed by the group of Janos Kirz and Chris Jacobsen at SUNY Stony Brook, with support from the Office of Biological and Environmental Research, U.S. DOE, under contract DE-FG02-89ER60858, and the NSF under grants DBI-9605045 and ECS-9510499. The FTIR data were collected at U10B of the NSLS, supported by the U.S. DOE under the contract DE-AC02-98CH10886. Many thanks are owed to Eduardo Neves, Jim Petersen, Fernando Costa, and Manuel Arroyo-Kalin for supplying the samples, to Lindsey Keller and Jim Heyne for discussion about the embedding procedure, and to Yuanming Zhang for invaluable help with sectioning.

References

Accardi-Dey, A., and P. M. Gschwend (2002), Assessing the combined roles of natural organic matter and black carbon as sorbents in sediments, *Environ. Sci. Technol.*, *36*, 21–29.

Agren, H., O. Vahtras, and V. Carravetta (1995), Near-edge core photoabsorption in polyacenes: Model molecules for graphite, *Chem. Phys.*, *196*, 47–58.

Bird, M. I., C. Moyo, E. M. Veendaal, J. Lloyd, and P. Frost (1999), Stability of elemental carbon in a savanna soil, *Global Biogeochem. Cycles*, *13*, 923–932.

Bradley, J. P., L. Keller, K. L. Thomas, T. B. Vander Wood, and D. E. Brownlee (1993), Carbon analyses of IDPs sectioned in sulfur and supported on beryllium films, in *24th Lunar and Planetary Sciences Conference*, edited by D. Blanchard and D. Black, pp. 173–174, Lunar and Planet. Inst., Houston, Tex.

Braida, W. J., J. J. Pignatello, Y. Lu, P. I. Ravikovitch, A. V. Neimark, and B. Xing (2003), Sorption hysteresis of benzene in charcoal particles, *Environ. Sci. Technol.*, *37*, 409–417.

Braun, A., N. Shah, F. E. Huggins, G. P. Huffman, S. Wirick, C. Jacobsen, K. Kelly, and A. F. Sarofim (2004), A study of diesel PM with X-ray microspectroscopy, *Fuel*, *83*, 997–1000.

Braun, A., F. E. Huggins, N. Shah, Y. Chen, S. Wirick, S. B. Mun, C. Jacobsen, and G. P. Huffman (2005), Advantages of soft X-ray absorption over TEM-EELS for solid carbon studies—A comparative study on diesel soot with EELS and NEXAFS, *Carbon*, *43*, 117–124.

Chen, J., B. Gu, E. J. LeBoeuf, H. Pan, and S. Dai (2002), Spectroscopic characterization of the structural and functional properties of natural organic matter fractions, *Chemosphere*, *48*, 59–68.

Cody, G. D., R. E. Botto, H. Ade, S. Behal, M. Disko, and S. Wirick (1995), Inner-shell spectroscopy and imaging of a subbituminous coal: In-situ analysis of organic and inorganic microstructure using C (1s)-, Ca (2p)-, and Cl (2s)-NEXAFS, *Energy Fuels*, *9*, 525–533.

Cody, G. D., H. Ade, S. Wirick, G. D. Mitchell, and A. Davis (1998), Determination of chemical-structural changes in vitrinite accompanying luminescence alteration using C-NEXAFS analysis, *Org. Geochem.*, *28*, 441–455.

Comelli, G., J. Stöhr, C. J. Robinson, and W. Jark (1988), Structural studies of argon-sputtered amorphous carbon films by means of extended X-ray-absorption fine structure, *Phys. Rev. B*, *38*, 7511–7519.

Decesari, S., M. C. Facchini, E. Matta, M. Mircea, S. Fuzzi, A. R. Chughtai, and D. M. Smith (2002), Water soluble organic compounds formed by oxidation of soot, *Atmos. Environ.*, *36*, 1827–1832.

Denley, D., P. Perfetti, R. S. Williams, D. A. Shirley, and J. Stöhr (1980), Carbon K-edge fine structure in graphite foils and in thin-film contaminants on metal surfaces, *Phys. Rev. B*, *21*, 2267–2273.

Dickens, A. F., Y. Gélinas, C. A. Masiello, S. Wakeham, and J. I. Hedges (2004), Reburial of fossil organic carbon in marine sediments, *Nature*, *427*, 336–339.

Flynn, G. F., L. P. Keller, C. Jacobsen, and S. Wirick (2004), As assessment of the amount and types of organic matter contributed to the Earth by interplanetary dust, *Adv. Space Res.*, *33*, 57–66.

Francis, J. T., and A. P. Hitchcock (1992), Inner-shell spectroscopy of p-benzoquinone, hydroquinone, and phenol: Distinguishing quinoid and benzenoid structures, *J. Phys. Chem.*, *96*, 6598–6610.

Gelinas, Y., K. M. Prentice, J. A. Baldock, and J. I. Hedges (2001), An improved thermal oxidation method for the quantification of soot/graphitic black carbon in sediments and soils, *Environ. Sci. Technol.*, *35*, 3519–3525.

Ghosh, U., J. S. Gilette, R. G. Luthy, and R. N. Zare (2000), Microscale location, characterization, and association of polycyclic aromatic hydrocarbons on harbor sediment particles, *Environ. Sci. Technol.*, *34*, 1729–1736.

Glaser, B., and W. Amelung (2003), Pyrogenic carbon in native grassland soils along a climosequence in North America, *Global Biogeochem. Cycles*, *17*(2), 1064, doi:10.1029/2002GB002019.

Glaser, B., L. Haumaier, G. Guggenberger, and W. Zech (2001), The Terra Preta phenomenon—A model for sustainable agriculture in the humid tropics, *Naturwissenschaften*, *88*, 37–41.

Guo, Y., and R. M. Bustin (1998), FTIR spectroscopy and reflectance of modern charcoals and fungal decayed woods: Implications for studies of inertinite in coals, *Int. J. Coal Geol.*, *37*, 29–53.

Gustafsson, Ö., T. D. Bucheli, Z. Kukulska, M. Andersson, C. Largeau, J.-N. Rouzaud, C. M. Reddy, and T. I. Eglinton (2001), Evaluation of a protocol for the quantification of black carbon in sediments, *Global Biogeochem. Cycles*, *15*, 881–890.

Haberhauer, G., B. Rafferty, F. Strebl, and M. H. Gerzabek (1998), Comparison of the composition of forest soil litter derived from three different sites at various decompositional stages using FTIR-spectroscopy, *Geoderma*, *83*, 331–342.

Hofrichter, M., D. Ziegenhagen, S. Sorge, R. Ullrich, F. Bublitz, and W. Fritsche (1999), Degradation of lignite (low-rank coal) by lignolytic basidiomycetes and their peroxidase system, *Appl. Microbiol. Biotechnol.*, *52*, 78–84.

Jacobsen, C., S. Wirick, G. Flynn, and C. Zimba (2000), Soft X-ray spectroscopy from image sequences with sub-100 nm spatial resolution, *J. Microsc.*, *197*, 173–184.

Koch, A., A. Krzton, G. Finqueneisel, O. Heintz, J. V. Weber, and T. Zimny (1998), A study of carbonaceous char oxidation in air by semi-quantitative FTIR spectroscopy, *Fuel*, *77*, 563–569.

Kuhlbusch, T. A. J., and P. J. Crutzen (1995), Toward a global estimate of black carbon in residues of vegetation fires representing a sink of atmospheric CO_2 and a source of O_2, *Global Biogeochem. Cycles*, *9*, 491–501.

Lehmann, J., D. C. Kern, L. German, J. McCann, G. C. Martins, and A. Moreira (2003a), Soil fertility and production potential, in *Amazonian Dark Earths: Origin, Properties, Management*, edited by J. Lehmann et al., pp. 105–124, Springer, New York.

Lehmann, J., D. C. Kern, B. Glaser, and W. I. Woods (Eds.) (2003b), *Amazonian Dark Earths: Origin, Properties, Management*, 505 pp., Springer, New York.

Lerotic, M., C. Jacobsen, T. Schäfer, and S. Vogt (2004), Cluster analysis of soft X-ray spectromicroscopy data, *Ultramicroscopy*, *100*, 35–57.

Lu, X. Q., L. V. Hanna, and W. D. Johnson (2001), Evidence of chemical pathways of humification: A study of aquatic humic substances heated at various temperatures, *Chem. Geol.*, *177*, 249–264.

Luo, Y., H. Agren, and F. Gel'mukhanov (1995), Symmetry-selective resonant inelastic X-ray scattering of C_{60}, *Phys. Rev. B*, *52*, 14,479–14,496.

Masiello, C. A., E. R. M. Druffel, and M. A. Currie (2002), Radiocarbon measurements of black carbon in aerosols and ocean sediments, *Geochim. Cosmochim. Acta*, *66*, 1025–1036.

Matrajt, G., G. J. Flynn, J. Bradley, and M. Maurette (2001), FTIR and STXM detection of organic carbon in scoriaceous-type antarctic micrometeorites, paper presented at 32nd Lunar and Planetary Sciences Conference, Lunar and Planet. Inst., Houston, Tex.

Mitra, S., T. S. Bianchi, B. A. McKee, and M. Sutula (2002), Black carbon from the Mississippi River: Quantities, sources, and potential implications for the global carbon cycle, *Environ. Sci. Technol.*, *36*, 2296–2302.

Neves, E. G., J. B. Peterson, R. N. Bartone, and C. A. da Silva (2003), Historical and socio-cultural origins of Amazonian dark earths, in *Amazonian Dark Earths: Origin, Properties, Management*, edited by J. Lehmann et al., pp. 29–50, Springer, New York.

Palotas, A. B., L. C. Rainey, C. J. Feldermann, A. F. Sarofim, and J. B. Vander Sande (1996), Soot morphology: An application of image analysis in high-resolution transmission electron microscopy, *Microsc. Res. Technol.*, *33*, 266–278.

Pessenda, L. C. R., S. E. M. Gouveia, and R. Aravena (2001), Radiocarbon dating of total soil organic matter and humin fraction and its comparison with ^{14}C ages of fossil charcoal, *Radiocarbon*, *43*, 595–601.

Pietikäinen, J., O. Kiikkilä, and H. Fritze (2000), Charcoal as a habitat for microbes and its effects on the microbial community of the underlying humus, *Oikos*, *89*, 231–242.

Pradhan, B. K., and N. K. Sandle (1998), Effect of different oxidizing agent treatments on the surface properties of activated carbons, *Carbon*, *37*, 1323–1332.

Rethemeyer, J., B. John, T. Yamashita, H. Flessa, G. Wiesenberg, L. Schwark, C. Kramer, G. Gleixner, M. J. Nadeau, and P. M. Grootes (2003), C dynamics in physical and chemical soil organic matter fractions investigated by AMS radiocarbon measurements, paper presented at Mechanisms and Regulation of Organic Matter Stabilisation in Soils: An International Conference, Dtsch. Forsch., Munich, Germany.

Rivera-Utrilla, J., I. Baulista-Toledo, M. A. Ferro-Garcia, and C. Moreno-Castilla (2001), Activated carbon surface modifications by adsorption of bacteria and their effect on aqueous lead adsorption, *J. Chem. Technol. Biotechnol.*, *76*, 1209–1215.

Schäfer, T., N. Hertkorn, R. Artinger, F. Claret, and A. Bauer (2003), Functional group analysis of natural organic colloids and clay association kinetics using C(1s) spectromicroscopy, *J. Phys. France*, *104*, 409–412.

Schäfer, T., G. Buckau, R. Artinger, S. Geyer, W. F. Bleam, S. Wirick, and C. Jacobsen (2005), Origin and mobility of fulvic acids in the Gorleben Aquifer system: Implications from isotopic data and carbon/sulfur XANES, *Org. Geochem.*, in press.

Scheinost, A. C., R. Kretzschmar, I. Christl, and C. Jacobsen (2001), Carbon group chemistry of humic and fulvic acid: A comparison of C-1s NEXAFS and ^{13}C-NMR spectroscopies, in *Humic Substances: Structures, Models and Functions*, edited by E. A. Ghabbour and G. Davies, pp. 39–47, R. Soc. of Chem., Gateshead, UK.

Schmidt, M. W. I. (2004), Biogeochemistry: Carbon budget in the black, *Nature*, *427*, 305–307.

Schmidt, M. W. I., and A. G. Noack (2000), Black carbon in soils and sediments: Analysis, distribution, implications, and current challenges, *Global Biogeochem. Cycles*, *14*, 777–794.

Schmidt, M. W. I., J. O. Skjemstad, E. Gehrt, and I. Kögel-Knabner (1999), Charred organic carbon in German chernozemic soils, *Eur. J. Soil Sci.*, *50*, 351–365.

Schmidt, M. W. I., J. O. Skjemstad, and C. Jäger (2002), Carbon isotope geochemistry and nanomorphology of soil black carbon: Black chernozemic soils in central Europe originate from ancient biomass burning, *Global Biogeochem. Cycles*, *16*(4), 1123, doi:10.1029/2002GB001939.

Shindo, H. (1991), Elementary composition, humus composition, and decomposition in soil of charred grassland plants, *Soil Sci. Plant Nutr.*, *37*, 651–657.

Shneour, E. A. (1966), Oxidation of graphitic carbon in certain soils, *Science*, *151*, 991–992.

Skjemstad, J. O., P. Clarke, J. A. Taylor, J. M. Oades, and S. G. McClure (1996), The chemistry and nature of protected carbon in soil, *Aust. J. Soil Res.*, *34*, 251–271.

Skjemstad, J. O., P. Clarke, A. Golchin, and J. M. Oades (1997), Characterization of soil organic matter by solid-state ^{13}C NMR spectroscopy, in *Driven by Nature*, edited by G. Cadisch and K. E. Giller, pp. 253–271, CAB Int., Wallingford, UK.

Skjemstad, J. O., J. A. Taylor, and R. J. Smernik (1999), Estimation of charcoal (char) in soils, *Commun. Soil Sci. Plant Anal.*, *30*, 2283–2298.

Skjemstad, J. O., D. C. Reicosky, A. R. Wilts, and J. A. McGowen (2002), Charcoal carbon in U.S. agricultural soils, *Soil Sci. Soc. Am. J.*, *66*, 1249–1255.

Skjemstad, J. O., L. P. Spouncer, B. Cowie, and R. S. Swift (2004), Calibration of the Rothamsted organic carbon turnover model (RothC ver. 26.3), using measurable soil organic carbon pools, *Aust. J. Soil Res.*, *42*, 79–88.

Smith, D. M., and A. R. Chughtai (1995), The surface structure and reactivity of black carbon, *Colloids Surf. A*, *105*, 47–77.

Soil Survey Staff (1997), *Keys to Soil Taxonomy*, 7th ed., *SMSS Tech. Monogr. Ser.*, vol. 19, Pocahontas, Blacksburg, Va.

Solomon, D., J. Lehmann, J. Kinyangi, B. Liang, and T. Schäfer (2005), Carbon K-edge NEXAFS and FTIR-ATR spectroscopic investigation of organic carbon speciation in soils, *Sci. Soc. Am. J.*, *69*, 107–119.

Sombroek, W. G., F. O. Nachtergaele, and A. Hebel (1993), Amounts, dynamics and sequestering of carbon in tropical and subtropical soils, *Ambio*, *22*, 417–426.

Steudel, R., and B. Eckert (2003), Solid sulfur allotropes, *Top. Curr. Chem.*, *230*, 1–79.

Stevenson, F. J., and M. A. Cole (1999), *Cycles of Soil: Carbon, Nitrogen, Phosphorus, Sulfur, Micronutrients*, 2nd ed., 427 pp., John Wiley, Hoboken, N. J.

Stöhr, J. (1992), *NEXAFS Spectroscopy*, *Ser. Surf. Sci.*, vol. 25, 403 pp., Springer, New York.

Vose, R. S., R. L. Schmoyer, P. M. Steurer, T. C. Peterson, R. Heim, T. R. Karl, and J. Eischeid (1992), The Global Historical Climatology Network: Long-term monthly temperature, precipitation, sea level pressure, and station pressure data, *ORNL/CDIAC-53*, Carbon Dioxide Inf. Anal. Cent., Oak Ridge Natl. Lab., Oak Ridge, Tenn.

Watson, R. T., R. Noble, B. Bolin, N. H. Ravindranath, D. J. Verardo, and D. J. Dokken (2000), *Land Use, Land-Use Change, and Forestry: Intergovernmental Panel on Climatic Change Special Report*, 375 pp., Cambridge Univ. Press, New York.

Wesner, D., et al. (1983), Synchrotron-radiation studies of the transition of hydrogenated amorphous carbon to graphitic carbon, *Phys. Rev. B*, *28*, 2152–2156.

C. Jacobsen, M. Lerotic, and S. Wirick, Department of Physics and Astronomy, State University of New York at Stony Brook, Stony Brook, NY 11794, USA.

J. Kinyangi, J. Lehmann, B. Liang, and D. Solomon, Department of Crop and Soil Sciences, Cornell University, 909 Bradfield Hall, Ithaca, NY 14853, USA. (cl273@cornell.edu)

F. Luizão, Instituto Nacional de Pesquisa da Amazonia INPA, Manaus, Brazil.

T. Schäfer, Forschungszentrum Karlsruhe, Institute für Nukleare Entsorgung (INE), P.O. Box 3640, D-76021 Karlsruhe, Germany.